Supplementary information

S1 Required output

Two simulations are required: one present day and one pre-industrial. If the simulations are nudged to present day meteorology, five years for each is sufficient. A list of required variables is given in Tab. S1.

5 S2 The RFari

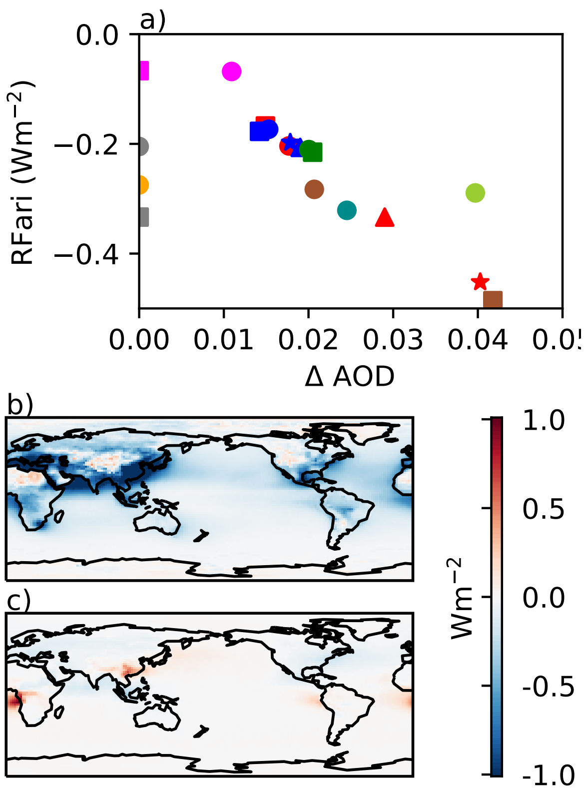

Figure S1. a) The change in AOD against the RFari (clear-sky), model icons are given in Table 1. b) The ensemble mean shortwave RFari (clear-sky). c) The mean shortwave RFari (cloudy-sky) for the AeroCom models.

The RFari is closely related to the change in the AOD (Fig. S1a), with an overall correlation between the RFari and the mean change in AOD of −0.76. The harmonized emissions from the AeroCom models (red, blue and green icons) produce a tight grouping of RFari estimates around $-0.2\,\mathrm{W\,m^{-2}}$, demonstrating the important role of the anthropogenic aerosol fraction. Although the role of surface albedo changes is generally small, it cannot always be neglected, almost doubling the RFari in the SPRINTARS model (SI Tab. S2). The impact of aerosol in overcast locations (RFari$_c$) is much smaller, averaging $+0.06\,\mathrm{W\,m^{-2}}$ in the AeroCom models. The CMIP5 models did not produce suitable output to calculate the RFari$_c$, but comparison to the absorbing component of the aerosol–cloud interaction in Zelinka et al. (2014) suggests that it is likely to also be small. The spatial patterns of the RFari and the RFari$_c$ are very different. The RFari (Fig. S1b) is strongest in regions of large aerosol perturbations, while the RFari$_c$ (Fig. S1c) is stronger in regions with large amounts of low-level liquid cloud. The overall mean estimate of $-0.2\,\mathrm{W\,m^{-2}}$ is smaller than the $-0.27\,\mathrm{W\,m^{-2}}$ from Quaas et al. (2009), but some of this difference is due to the postive forcing from aerosol above clouds.

CMOR name	Long name/*Notes*
rsut	TOA outgoing shortwave (all-sky)
	All-sky albedo is an alternative
rsutcs	TOA outgoing shortwave (clear-sky)
	Clear-sky albedo is an alternative
clt	Total cloud cover
clwvi	Liquid water path
clivi	Ice water path
icc	Ice cloud cover
	Satellite simulated fraction
clhcalipso	CALIPSO simulator high cloud cover
	Alternative to icc
clmcalipso	CALIPSO simulator mid-level cloud cover
	Alternative to icc
lcc	Liquid cloud cover
	Satellite simulated fraction
cllcalipso	CALIPSO simulator low cloud cover
	Alternative to lcc
rlut	TOA Outgoing longwave radiation (all-sky)
	Longwave/ice decomposition only
rlutcs	TOA Outgoing longwave radiation (clear-sky)
	Longwave/ice decomposition only
rsdt	TOA incoming shortwave
	Can be calculated offline
	Not required if albedos used
rsutnoa	rsut but with aerosol not active in radiation
rsutcsnoa	rsutcs but with aerosol not active in radiation
	Required for above-cloud aerosol
rsdscs	Downwelling shortwave at surface
	Required for surface if rsutcsnoa unavailable
rsuscs	Upwelling shortwave at surface
	Required for surface if rsutcsnoa unavailable
od550aer	Aerosol optical depth at 550nm
	Analysis only, not required for decomposition

Table S1. Required output variables for the decomposition

Model	ΔSW	Surf.	RFari$_{cs}$	RFari$_{c}$	$\Delta\alpha_l$	$\Delta\alpha_i$	Δf_l	Δf_i	Res
ECHAM6-HAM2.2	−1.89	−0.01	−0.20	0.03	−0.94	−0.17	−0.17	−0.42	−0.01
-CND	−0.94	0.00	−0.17	-	−0.45	−0.10	0.18	−0.37	−0.03
-anthsca1.5	−2.33	0.00	−0.33	-	−1.09	−0.20	−0.19	−0.49	−0.03
-anthsca2	−2.80	0.00	−0.45	-	−1.28	−0.24	−0.23	−0.58	−0.02
-anthsca4	−4.24	0.00	−0.89	-	−1.83	−0.35	−0.36	−0.82	0.01
HadGEM3-UKCA	−2.74	-	−0.45	-	−1.29	−0.45	−0.18	−0.07	−0.30
CAM5.3	−2.10	0.01	−0.17	0.12	−1.13	−0.22	−0.68	−0.06	0.04
CAM5.3-MG2	−1.55	−0.01	−0.18	0.08	−1.29	0.00	−0.11	0.05	−0.08
CAM5.3-CLUBB	−2.44	0.00	−0.21	0.11	−1.22	−0.22	−0.97	−0.05	0.12
CAM5.3-CLUBB-MG2	−2.47	0.00	−0.20	0.08	−1.44	−0.02	−0.64	−0.42	0.16
SPRINTARS	−1.18	−0.18	−0.21	−0.03	−0.68	−0.05	−0.06	−0.00	0.03
SPRINTARS-KK	−1.46	−0.19	−0.22	−0.03	−0.79	−0.06	−0.15	−0.00	−0.01
CanESM2	−0.95	−0.01	−0.27	-	−0.47	−0.17	−0.06	0.03	0.01
HadGEM2-A	−1.33	0.02	−0.28	-	−0.76	−0.19	−0.27	0.06	0.10
IPSL-CM5A-LR	−0.53	−0.03	−0.29	-	−0.07	−0.07	−0.07	0.00	−0.00
MIROC5	−1.78	−0.05	−0.32	-	−1.16	−0.36	−0.23	0.00	0.33
MRI-CGCM3-p1	−2.06	0.03	−0.07	-	−0.82	−0.98	−0.05	−0.39	0.22
MRI-CGCM3-p3	−2.63	0.03	−0.07	-	-	-	-	-	-
MPI-ESM-LR-p1	−0.24	−0.01	−0.20	-	-	-	-	-	-
MPI-ESM-LR-p3	−0.43	−0.05	−0.33	-	-	-	-	-	-
Mean	−1.82	−0.02	−0.28	0.05	−0.93	−0.27	−0.25	−0.21	0.03
S.D.	0.96	0.06	0.17	0.09	0.43	0.31	0.27	0.26	0.13

Table S2. The SW decomposition. The column “Res” is the residual from the decomposition into changes in cloud albedo “$\Delta\alpha_c$” and cloud fraction Δf_c. Values are given in W m^{-2}, with a negative indicating a negative radiative forcing (a cooling effect). Dashes indicate insufficient output for the decomposition, these components are assumed zero in calculating the residuals. CMIP5 values assume no impact of aerosol above cloud.

Model	ΔLW	RFari$_{cs}$	dLW$_l$	dLW$_i$	dLW$_{f_l}$	dLW$_{f_i}$	Res
ECHAM6-HAM2.2	0.83	0.01	−0.04	0.42	0.03	0.46	−0.05
-CND	0.53	−0.03	−0.08	0.31	−0.07	0.42	−0.02
-anthsca1.5	0.85	0.01	−0.10	0.41	0.04	0.56	−0.07
-anthsca2	1.00	0.02	−0.12	0.48	0.05	0.67	−0.10
-anthsca4	1.43	0.06	−0.22	0.65	0.08	0.98	−0.11
HadGEM3-UKCA	0.44	0.11	0.09	0.25	0.06	0.05	−0.12
CAM5.3	0.69	0.09	−0.07	0.58	0.19	0.07	−0.17
CAM5.3-MG2	0.25	0.05	0.01	0.35	0.10	−0.04	−0.22
CAM5.3-CLUBB	0.70	0.10	−0.08	0.56	0.29	0.05	−0.21
CAM5.3-CLUBB-MG2	0.82	0.12	0.03	0.11	0.21	0.34	0.01
SPRINTARS	0.19	0.07	0.01	0.09	0.02	0.00	−0.00
SPRINTARS-KK	0.23	0.08	0.00	0.12	0.05	0.01	−0.02
CanESM2	0.07	0.06	0.04	−0.05	0.02	−0.02	0.02
HadGEM2-A	0.09	0.08	0.06	−0.00	0.04	−0.06	−0.02
IPSL-CM5A-LR	−0.21	0.02	−0.01	−0.02	0.02	−0.00	−0.22
MIROC5	0.49	0.12	0.06	0.25	0.06	0.03	−0.03
MRI-CGCM3	0.96	0.00	0.01	0.59	0.01	0.34	0.00
MRI-CGCM3	1.15	0.00	-	-	-	-	-
MPI-ESM-LR	−0.12	−0.01	-	-	-	-	-
MPI-ESM-LR	−0.20	−0.02	-	-	-	-	-
Mean	0.51	0.05	−0.02	0.30	0.07	0.23	−0.07
S.D.	0.45	0.05	0.08	0.22	0.08	0.30	0.08

Table S3. As Tab. S2, but the LW decomposition. The final column shows the residual from the decomposition. Values are in $\mathrm{W\,m^{-2}}$.

Model	N_d	$\mathscr{L}$	f_c	f_c(corr)	$\mathscr{L}$ (%)	f_c(%)	f_c(corr, %)
ECHAM6-HAM2.2	−0.45	−0.50	−0.17	−0.29	110	37	64
-CND	−0.42	−0.02	0.18	0.07	6	−43	−17
-anthsca1.5	−0.47	−0.61	−0.19	−0.33	129	40	70
-anthsca2	−0.56	−0.72	−0.23	−0.39	128	40	70
-anthsca4	−0.78	−1.05	−0.36	−0.60	134	46	76
HadGEM3-UKCA	−1.28	−0.01	−0.18	−0.19	1	14	15
CAM5.3	−0.82	−0.31	−0.68	−0.70	38	83	85
CAM5.3-MG2	−0.97	−0.32	−0.11	−0.07	33	12	7
CAM5.3-CLUBB	−0.76	−0.46	−0.97	−0.99	61	128	130
CAM5.3-CLUBB-MG2	−0.90	−0.55	−0.64	−0.81	61	71	90
SPRINTARS	−0.65	−0.03	−0.06	−0.06	5	10	9
SPRINTARS-KK	−0.66	−0.13	−0.15	−0.15	20	23	23
CanESM2	−0.45	−0.03	−0.06	−0.05	6	13	12
HadGEM2-A	−0.68	−0.09	−0.27	−0.25	13	40	36
IPSL-CM5A-LR	−0.08	0.01	−0.07	−0.06	−10	88	71
MIROC5	−1.07	−0.09	−0.23	−0.26	8	22	24
MRI-CGCM3	−0.73	−0.09	−0.05	−0.14	13	8	19

Table S4. The decomposition of the liquid cloud albedo change into $\mathscr{L}$ and N_d (RFaci) changes. The forcing from liquid cloud fraction changes is shown along with a forcing assuming no ice cloud fraction changes. Values are in $\mathrm{W\,m^{-2}}$.